Quantitative analysis of nucleoside transporter and metabolism gene expression in chronic lymphocytic leukemia (CLL): identification of fludarabine-sensitive and -insensitive populations

John R. Mackey, Carlos M. Galmarini, Kathryn A. Graham, Anil A. Joy, Alain Delmer, Laith Dabbagh, Darryl Glubrecht, Lawrence D. Jewell, Raymond Lai, Thack Lang, John Hanson, James D. Young, Helene Merle-Béral, Jacques L. Binet, Carol E. Cass, and Charles Dumontet

Resistance to fludarabine is observed in the clinic, and molecular predictive assays for benefit from chemotherapy are required. Our objective was to determine if expression of nucleoside transport and metabolism genes was associated with response to fludarabine therapy in patients with chronic lymphocytic leukemia (CLL). CLL cells from 56 patients were collected prior to treatment with fludarabine. Quantitative reverse transcriptase–polymerase chain reaction (RT-PCR) was performed on sample RNA to determine the relative levels of mRNA of 3 nucleoside transporters that mediate fludarabine uptake (human equilibrative nucleoside transporter 1 [hENT1], human equilibrative nucleoside transporter 2 [hENT2], and human concentrative nucleoside transporter 3 [hCNT3]), deoxycytidine kinase (dCK), and 3 5′-nucleotidases (ecto-5′nucleotidase [CD73], deoxynucleotidase-1 [dNT-1], and cytoplasmic high-K_m 5-nucleotidase [CN-II]). Two-dimensional hierarchical cluster analysis of gene expression identified 2 distinct populations of CLL. Cluster 2 patients experienced a 3.4-fold higher risk of disease progression than cluster 1 patients ($P = .0058$, log-rank analysis). Furthermore, independent analysis of the individual genes of interest revealed statistically significant differences for risk of disease progression (adjusted hazard ratios [HRs]) with underexpression of dNT-1 (HR = 0.45; $P = .042$), CD73 (HR = 0.40; $P = .022$), and dCK (HR = 0.0.48; $P = .035$), and overexpression of hCNT3 (HR = 4.7; $P = .0007$) genes. Subjects with elevated hCNT3 expression experienced a lower complete response rate to fludarabine therapy (11% vs 69%; $P = .002$). No hCNT3-mediated plasma membrane nucleoside transport was detected in CLL samples expressing hCNT3 message, and hCNT3 protein was localized to the cytoplasm with immunohistochemical and confocal microscopy. (Blood. 2005;105:767-774)

© 2005 by The American Society of Hematology

Introduction

Chronic lymphocytic leukemia (CLL) is the most common hematologic malignancy and occurs in a predominantly elderly population. The nucleoside antimetabolite fludarabine (9-β-D-arabinosyl-2-fluoroadenine) is one of several cytotoxic agents used in the treatment of CLL. Fludarabine monotherapy produces responses in 63% to 79% of untreated patients and 32% to 48% of pretreated patients.[1-7] Although initial treatment of CLL with fludarabine yields higher response rates, a longer duration of remission, and longer progression-free survival than initial treatment with chlorambucil,[3] no survival advantage has been convincingly demonstrated for fludarabine-treated patients. Fludarabine nonresponders are at risk for the potentially serious complications of therapy (myelosuppression, hemolytic anemia) and incur the pharmacoeconomic costs of ineffective drug therapy. Presently, there is no validated means to predict clinical benefit in CLL patients treated with fludarabine chemotherapy.

Fludarabine is an analog of adenosine and has activity against both actively dividing and resting cells via multiple cytotoxic mechanisms.[8-12] Although resistance to fludarabine may occur by several means, one proposed mechanism of cellular and clinical resistance is reduced intracellular drug accumulation.[13] The early steps of plasma membrane transport, nucleoside phosphorylation, and nucleotide dephosphorylation determine intracellular accumulation of fludarabine and its metabolites. Fludarabine is administered as the 5′-nucleotide monophosphate and is converted to the nucleoside by the activity of serum phosphatase and ecto-5′nucleotidase (CD73). As fludarabine is a hydrophilic compound and does not readily cross plasma membranes by diffusion, the presence of functional nucleoside transporters that accept fludarabine as a permeant is required for cellular entry at rates sufficient to achieve cytotoxic levels of intracellular metabolites. Three human (h) nucleoside transporter proteins, equilibrative nucleoside transporter 1 (hENT1), equilibrative nucleoside transporter 2 (hENT2), and concentrative nucleoside transporter 3 (hCNT3), have been shown to mediate cellular entry of fludarabine.[14-16] Ex vivo, the accumulation of fludarabine in CLL cells was recently reported to be mediated exclusively by ENT-type transporters.[16]

Within the cell, fludarabine requires anabolism to the active 5′-triphosphate (fludarabine triphosphate) to exert its cytotoxic effects. The rate-limiting step in this process is the conversion by

deoxycytidine kinase (dCK) of free nucleoside to the 5′-nucleotide monophosphate.[17] Directly opposing dCK activity are the intracellular 5′-nucleotidases, including the high-K_m 5′-nucleotidase (CN-II) and deoxynucleotidase-1 (dNT-1).[13]

In order to identify molecular markers of potential predictive value in CLL, we studied CLL patients who had not previously been treated with fludarabine to determine the cellular expression of genes encoding nucleoside transporter proteins and enzymes mediating fludarabine metabolism. We then analyzed the relationships between RNA expression and time to disease progression following fludarabine therapy.

Patients, materials, and methods

Patients

A total of 56 CLL patients were treated in the Hematology Departments of Hôpital La Pitié, Edouard Herriot, and Saint Louis in France. The diagnosis of classic B-cell CLL was made by standard cytologic and histologic examination of peripheral blood and bone marrow smears, and patients were staged according to the Binet classification system for CLL.[18] None of the patients had circulating prolymphocyte cells in an abundance that exceeded 10% of lymphocytes. Approval was obtained from Lyon Protocol Review Board and the Cross Cancer Institute Research Ethics Committee. Written informed consent was provided by all study subjects.

Treatment and efficacy assessment

Fludarabine was administered with the standard schedule and dosage of 25 mg/m² intravenously over a period of 10 to 30 minutes on days 1 through 5 every 28 days for 6 cycles or until disease progression. The number of cycles delivered, the time to disease progression, and overall survival data were obtained for each participant. Time to disease progression (TDP), which was calculated from the date of initiation of fludarabine therapy until the date of disease progression or death, was chosen as the primary end point of this study because it could be determined more reliably than the objective response rate. Progression of disease was defined by the presence of at least one of the following[19]: (a) increase of absolute lymphocyte count by at least 50% to at least 10×10^9/L from the nadir reached during therapy, over 2 consecutive examinations at least 2 weeks apart; (b) increase by at least 50% in the sum of area of all nodes or appearance of new nodal involvement; (c) increase by at least 50% in the span of the liver or spleen below costal margin; (d) transformation to a more aggressive histology, such as Richter syndrome; (e) development of idiopathic thrombocytopenic purpura without other obvious cause. For those patients surviving without disease progression, TDP was censored at the time of last follow-up.

Chronic lymphocytic leukemia cells

All samples were obtained prior to initiation of fludarabine chemotherapy. Peripheral blood was collected in heparinized tubes, and mononuclear cells were isolated by Ficoll-Hypaque sedimentation.

Quantitative real-time RT-PCR

The relative level of mRNA encoding nucleoside transporters (hENT1, hENT2, hCNT3), nucleotidases (dNT1, CN-II, CD73), and dCK was assessed by quantitative real-time polymerase chain reaction (PCR; ABI PRISM 7700 Sequence Detection System [TaqMan]; Applied Biosystems, Foster City, CA). The probe and primers used in the TaqMan reactions were designed using Primer Express software (Applied Biosystems, Camarillo, CA; Table 1). From each CLL sample, total cellular RNA was extracted from 10^7 cells using the RNeasy Mini Protocol (QIAGEN, Mississauga, ON, Canada). RNA was then reverse transcribed using the TaqMan Gold reverse transcriptase–PCR (RT-PCR) Kit (Applied Biosystems, Foster City, CA) according to the manufacturer's protocols. Briefly, RT reaction mixtures consisted of total RNA (200 ng), $1 \times$ TaqMan RT buffer (Applied

Table 1. Nucleic acid sequences of primers and probes used in quantitative RT-PCR reactions

Accession no. and oligonucleotide	Sequence
U81375	
hENT1-F	5′-CACCAGCCTCAGGACAGATACAA
hENT1-R	5′-GTGAAATACTGAGTGGCCGTCAT
hENT1-P	5′-FAM-CCACGGGAGCAGCGTTCCCA
U81375	
hENT2-F	5′-ATGAGAACGGGATTCCCAGTAG
hENT2-R	5′-GCTCTGATTCCGGCTCCTT
hENT2-P	5′-TET-CAGAAAGTAGCTCTGACCCTGGATCTTGACCT
AF305210	
hCNT3-F	5′-GGGTCCCTAGGAATCGTGATC
hCNT3-R	5′-CGAGGCGATATCACGCTTTC
hCNT3-P	5′-FAM-CGGACTCACATCCATGGCTCCTTC
M60527	
dCK-F	5′-AAACCTGAACGATGGTCTTTTACC
dCK-R	5′-CTTTGAGCTTGCCATTCAGAGA
dCK-P	5′-FAM-CAAACATATGCCTGTCTCAGTCGAATAAGAGCTC
NM_002526	
CD73-F	5′-TCCGGTCGCCCATTGA
CD73-R	5′-GCCTCCAAAGGGCAATACAG
CD73-P	5′-FAM-ACGCAACAATGGCACAATTACCTGGG
D38524	
CN-II-F	5′-ACCTGCTGTATTACCCTTTCAGCTA
CN-II-R	5′-GCTCCACCGTTGATTCATGA
CN-II-P	5′-FAM-CTCTTCAGGGCTGCCCATGTCTTGA
NM_014595	
dNT1-F	5′-GGACACGCAGGTCTTCATCTG
dNT1-R	5′-GCGGTACTTCTCACCCACACA
dNT1-P	5′-FAM-CCAGCCCCCTGCTGAAGTACCACC

F indicates forward (5′) primer; R, reverse (3′) primer; P, probe; FAM, 6-carboxy-fluorescein; and TET, tetrochloro-6-carboxy-fluorescein.

Biosystems), $MgCl_2$ (2.5 mM), random hexamer (2.5 μM), RNase inhibitor (0.4 U/ μL), deoxyNTPs mixture (500 μM each), MultiScribe reverse transcriptase (1.23 U/μL), and RNase-free H_2O to a total volume of 10 μL. Reaction mixtures were prewarmed at 25°C for 10 minutes, incubated at 48°C for 30 minutes, and subsequently heated to 95°C for 5 minutes to terminate the reaction. The resulting cDNAs were subjected to real-time PCR and analyzed with a 7700 Sequence Detection System. The TaqMan Universal PCR Master Mix kit (Applied Biosystems) was used to prepare the reactions for real-time PCR. Briefly, cDNAs (2 μL) were mixed with $2 \times$ Universal PCR Master Mix (25 μL), primers (300 μM each), and probe (100 μM) in a total volume of 50 μL. These reactions were prepared in duplicate. Cycling conditions were the manufacturer's recommended default values (1 cycle of 2 minutes at 50°C and 10 minutes at 95°C, then 40 cycles of 15 s at 95°C and 1 minute at 60°C).

Relative quantitation of mRNA levels was performed using glyceraldehyde phosphate dehydrogenase (GAPDH) as an internal control.[20] Validation assays[20] demonstrated that all of the genes included in this study were amplified with equal efficiency (data not shown). The results are expressed as C_T values, which are the PCR cycle numbers at which the accumulated fluorescent signal in each reaction crossed a threshold above background.[20] The C_T value obtained for a particular sample was corrected for RNA concentration by subtracting the C_T value for GAPDH (ΔC_T). The results were then normalized to the mRNA level in reference peripheral blood mononuclear cells from a single healthy control (reference ΔC_T − test $\Delta C_T = \Delta \Delta C_T$). The results were expressed as $2^{-(\Delta \Delta CT)}$ (arbitrary quantitative PCR units), as previously described.[15,20-22]

Cluster analysis of gene expression

For each of the 56 CLL patients, the results of the real-time RT-PCR assays (with values defined in arbitrary quantitative PCR units) were analyzed using the hierarchical gene clustering methods of the Cluster software

program (Stanford University, Stanford, CA).[23,24] In brief, the program organizes sets of data (eg, the 7 set mRNA profiles for each CLL patient) into groups of similar values. Hierarchical agglomerative clustering involves building a hierarchical classification of entities in a data set by a series of binary mergers (agglomerations), initially of individual entities and later of clusters formed at previous stages of the analysis. The results of the hierarchical clustering were displayed graphically in the form of a dendrogram using the TreeView program[23] (Stanford University) to indicate the nature of the computed relationships among gene coding sequences in the cluster analysis, where the dendrogram branch lengths reflect the degree of similarity between the clustered groups, and genes with similar expression patterns are adjacent to one another.

Gene expression relationships to clinical outcomes

Forty-five of the 56 CLL study population patients received fludarabine and had full clinical follow-up information available and this population is referred to as the treatment population. The treatment population was studied for relationships between gene expression, TDP, and associated clinical variables. The 2 primary clusters were studied using log-rank analysis of Kaplan-Meier time-to-progression curves.

For the purpose of statistical analysis of expression of individual genes, variables were dichotomized (high versus low levels), and the optimum separation was determined for each marker. Using real-time RT-PCR results for each of the 7 genes of interest (hENT1, hENT2, hCNT3, dCK, dNT-1, CN-II, CD73), Kaplan-Meier survival curves were constructed and log-rank tests were performed for a series of 2 predefined groups. The groups were classified as (a) those cases with values less than and (b) those cases with values greater than or equal to an optimal real-time RT-PCR value. The optimal value was taken as the one that maximized the significance of the difference between the groups according to the log-rank test and for which each group had at least 8 cases (the minimum number of cases in a group as previously determined in the cluster analysis groupings). The Kaplan-Meier method was used to determine TDP curves and comparisons made using the log-rank test. Cox survival analysis was used to determine significance levels and estimate hazard ratios (HRs) with 95% confidence intervals (95% CIs) for the optimum cut point groups. The hazard ratios were adjusted for the optimum cut point selection using methods described elsewhere.[25] Hazard ratios were considered significantly different if the P value was less than or equal to .05. Variables studied in the univariate and multivariate analyses included relative mRNA levels, sex, age, white blood cell (WBC) count, number of fludarabine courses, clinical treatment response, and hematologic treatment response.

To further explore the relationships between gene expression and fludarabine sensitivity, the mean RNA expression level of each of the 7 genes was compared between those patients who achieved complete response and those who did not achieve complete response, using 2-sided t testing. Results were considered significantly different if the P value was less than or equal to .05. Fisher exact analysis was performed to identify relationships between complete response and cluster designation, as well as complete response and gene expression using the optimized cut points.

Plasma membrane hCNT3 activity in CLL cells

Because hCNT3 expression correlated strongly with clinical outcome, we undertook studies to determine whether CLL cells had evidence of sodium-dependent plasma membrane uptake of a radiolabeled nucleoside. From a population of 21 CLL patients previously described,[22] we selected 3 fludarabine-naive patients whose CLL samples had the highest expression of hCNT3 message. Peripheral blood was collected in heparinized tubes. An equal volume of phosphate-buffered saline (PBS) was added to the blood and a portion of the resulting mixture was layered on the Ficoll-Paque (Pharmacia Biotech, Piscataway, NJ) solution. After centrifugation, cells at the interface were washed twice and resuspended in PBS. Suspension nucleoside transport studies were performed as previously described[22] for assay of sodium-dependent nucleoside uptake mediated by hCNT3. In brief, cells were washed twice with the appropriate transport buffer (Na$^+$ or N-methyl-D-glucamine) and then processed immediately or incubated with 100 μM dilazep at room temperature for 20 minutes

before the transport assay. Portions (100 μL) of [3-H]-uridine–containing permeant solution were layered on to 200 μL of transport oil, and transport assays were initiated by adding 100 μL portions of cell suspensions and were terminated at the appropriate time by adding 100 μL of ice-cold dilazep-containing solution (final concentration, 100 μM) and immediately centrifuging (16 000g). The supernatants were removed and discarded and the cell pellets were solubilized overnight in 500 μL of 5% Triton X-100. Cell-associated radioactivity was determined using liquid scintillation counting.

Immunohistochemistry of hCNT3 protein in CLL cells

An immunohistochemical assay to detect hCNT3 in clinical samples of CLL was developed using monoclonal antibodies raised against a synthetic hCNT3 peptide (conjugated to keyhole limpet hemocyanin) that corresponded to amino acid residues 45-69 of the predicted intracellular loop near the amino terminus of the protein. The origin and validation of these monoclonal anti-hCNT3 antibodies, named TL3360, are described elsewhere.[26] Goat antimouse antibodies and horseradish peroxidase–labeled dextran polymer (DAKO EnVision+) were from DAKO Corporation (Carpinteria, CA).

Formalin-fixed, paraffin-embedded lymph nodes derived from 16 individuals with CLL, and 3 samples of normal pancreas, were obtained from Cross Cancer Institute patients. Paraffin-embedded sections of 5-μm thickness were dried in an oven at 59°C for 2 hours. Sections were rehydrated through 3 changes of xylene, then through graded ethanol from 100% to 50%, then water (10 minutes per change). Slides were microwaved in a rapid microwave histoprocessor (RHS, Milestone, Bergamo, Italy) at a controlled final temperature of 100°C for 10 minutes in DAKO Tris (tris(hydroxymethyl)aminomethane) buffer (pH 9.9), cooled for 6 minutes, and washed in running cold tap water. Slides were incubated in 3% H_2O_2 in methanol for 10 minutes and rewashed for 5 minutes in tap water. Tissue sections were then incubated with 1:5 dilutions of the TL3360 anti-hCNT3 antibody preparations in a room temperature humidity chamber for 30 minutes. The sections were then rinsed in PBS (pH 7.2) and immersed in PBS for 5 minutes, incubated with Envision (DAKO EnVision+) goat antimouse dextran conjugate for 30 minutes, washed in PBS for 5 minutes, incubated with diamino-benzidene solution, rinsed, counter-stained with hematoxylin, dehydrated through graded alcohols and xylene, and cover-slipped. Negative controls were provided by either omitting the TL3360 primary antibodies, by using antibody preparations from which anti-hCNT3 antibodies had been removed by incubation with an excess of anti-hCNT3 peptide, or by substitution of primary antibodies with anti-CD38 monoclonal antibodies. Positive controls were provided by sections of pancreas, a tissue known to express high levels of hCNT3 message[15] and shown to have readily detectable membrane hCNT3 staining by immunohistochemistry. Immunohistochemistry was assessed and scored subjectively by a single pathologist (L.D.J.) blinded to clinical characteristics and outcomes.

Confocal microscopy for hCNT3 protein in CLL cells

Three samples from fludarabine-naive CLL were prepared as described in the previous section, and cytospin preparations were frozen and processed for confocal microscopy. All incubations were carried out at room temperature in a humidified chamber where applicable. Cells were fixed in paraformaldehyde (SIGMA, St Louis, MO; 4% in PBS, 10 minutes), rinsed in PBS (3 times, 5 minutes each), and permeabilized in Triton (0.1% in PBS, 10 minutes). The slides were then washed in PBS (3 times, 5 minutes each), blocked in goat serum (2% in PBS, 30 minutes), probed with the addition of hCNT3 monoclonal antibody (undiluted, 30 minutes), and washed in PBS (3 times, 5 minutes each). A secondary antibody, goat antimouse tagged with Alexa 488 (Molecular Probes, Eugene, OR; 1:250 in PBS, 30 minutes), was added to the slides, which were then washed with PBS (3 times, 5 minutes each) and mounted with 90% glycerol/10% PBS containing p-phenylendiamine (SIGMA) as an antifade agent and Dapi (4,6 diamidino-2-phenylindole; SIGMA) to stain the DNA. An immunoglobulin M (IgM) isotype control antibody (SIGMA) was also used. The cells were visualized using a Zeiss Axiovent 100M confocal microscope using a Zeiss

40 × lens with a 1.3 numerical aperture and Zeiss 510 LSM software (Thornwood, NY).

Results

Patient demographics and treatment outcome

Fifty-six fludarabine-naive CLL patients (the study population) participated in this investigation and supplied blood samples for RT-PCR analysis. Forty-five of the 56 CLL patients subsequently received fludarabine (the treated population) and had clinical outcomes, including number of fludarabine cycles administered, hematologic response, clinical response, time to progressive disease, and survival duration. These 45 patients consisted of 11 women and 34 men with a median age of 56 years (range, 32-76 years). The median number of courses received was 6 (range, 3 to 12). Twenty-three patients (51%) received 6 courses. Complete hematologic responses were observed in 31 patients, partial hematologic response in 9, and 5 subjects had no hematologic response. Complete clinical responses were observed in 30 patients, partial clinical response in 7 subjects, and 8 patients had no clinical response. Complete responses, defined as both a complete hematologic response and complete clinical response, were observed in 26 patients (58%). Partial responses, defined as at least a partial clinical response and at least a partial hematologic response but not complete response, were observed in 11 patients (24%). Eight subjects (18%) had no response to fludarabine therapy.

Relative levels of mRNA for nucleoside transport and metabolism genes

Relative levels of mRNA were determined for each of the 7 genes in all 45 samples from the treated population. The median and range of mRNA levels for the 7 genes, relative to those for the GAPDH gene, are listed in Table 2. Unsupervised cluster analysis of gene expression was performed on all 56 CLL study samples, and results are displayed graphically in Figure 1. Two primary clusters were identified, cluster 1 consisting of 37 patients and cluster 2 with 8 patients. The clinical outcomes of these 2 patient clusters differed markedly, as demonstrated by log-rank analysis of the outcomes of the treatment sample (Figure 2; Table 3). Study population patients in cluster 1 had a median TDP of 834 days, whereas patients in cluster 2 had a median TDP of 304 days (HR 3.4, $P = .0058$ by log-rank analysis; HR 3.97, $P = .0081$ by Cox regression). Study population patients in cluster 1 achieved a complete response to fludarabine in 25 (67%) of 37 cases, whereas
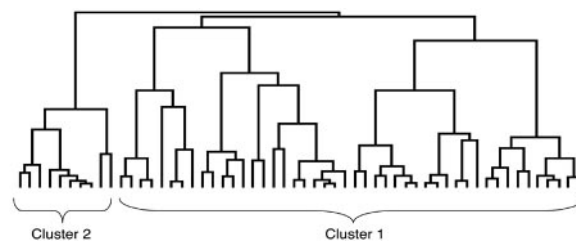

Figure 1. Dendrogram of cluster analysis. Fifty-six CLL samples from fludarabine-naive patients were analyzed for gene expression of 7 genes involved in fludarabine transport and metabolism. Uncentered hierarchical gene clustering analysis organized the samples displayed graphically in the form of a dendrogram. Samples with similar expression patterns of the 7 genes are adjacent to one another, and the dendrogram branch lengths reflect the degree of similarity between the clustered groups. Two major expression patterns (cluster 1 and cluster 2) are identified.

cluster 2 patients achieved a complete response in only 1 of 8 cases (13%; $P = .006$ by Fisher exact test). These cluster results were generated without supervision or incorporation of outcome data. This strongly suggests that the expression patterns of genes encoding nucleoside transporter proteins and enzymes of fludarabine metabolism intrinsically separated 2 populations of CLL patients that differed in fludarabine sensitivity, as well as in duration of benefit from fludarabine therapy. The cluster designation did not significantly correlate with the clinical parameters of patient age, stage, sex, or pretreatment lymphocyte counts (data not shown).

Gene expression relationship to clinical outcome

To determine which individual gene's expression most strongly correlated with clinical benefit from fludarabine, an exploratory analysis of each of the 7 genes was performed to determine the optimized cutoff that maximized the difference between dichotomized groups. The expression of hCNT3, dCK, CD73, and dNT-1 showed statistically significant associations with time to disease progression after fludarabine therapy on unadjusted analysis. However, when adjusted to account for the optimum cut point selection, only hCNT3 was retained as a significant predictor of TDP with a hazard ratio of 4.67 and 95% confidence limits for the hazard ratio that did not include unity (Table 3). No other gene dichotomy performed as well, although dichotomizing the treatment populations identified that higher levels of dCK, CD73, and dNT-1 expression conferred a trend to longer times to disease progression (adjusted HRs of 0.48, 0.40, and 0.45, respectively; Table 3). Thus, the single gene that most strongly related to clinical outcome was the fludarabine membrane transporter hCNT3 (Table 3; Figures 3-4). Patients with low hCNT3 mRNA levels had a

Table 2. Summary of relative levels of mRNA for nucleoside transport and metabolism genes

mRNA	No. of patients	Gene expression		
		Low	High	Median
hENT1	44	0.05	1.97	0.40
hENT2	45	0.24	837	1.15
hCNT3	45	0.01	2.41	0.12
dCK	45	0.86	161	4.47
CD73	45	0.00	39.7	0.43
CN-II	43	0.00	12.8	1.59
dNT-1	45	0.00	105	1.65

The C_T value obtained for a sample was corrected for RNA concentration by subtracting the C_T value for GAPDH (ΔC_T). The results were then normalized to the expression level in reference peripheral blood mononuclear cells derived from a single healthy donor (reference ΔC_T − test $\Delta C_T = \Delta\Delta C_T$) and expressed as $2^{-(\Delta\Delta CT)}$ (arbitrary quantitative PCR units) as previously described.[15,20,21]
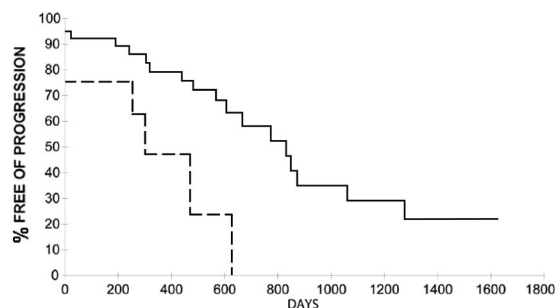

Figure 2. Time to disease progression dichotomized by cluster groupings. Kaplan-Meier analysis demonstrates that patients in cluster group 2 (- - -) had a shorter time to disease progression after fludarabine therapy compared with those in cluster group 1 (—). The difference is significant, with a hazard ratio of 3.4 ($P = .058$ by log-rank analysis). The hazard ratio is 3.97 ($P = .0081$ using Cox regression).

Table 3. Summary of results

| | | | | | HR of group 1/group 2 | | | |
Marker of interest	No. of patients (group 1/group 2)	Cutoff value	Median TDP group 1, less than cutoff, d	Median TDP group 2, greater than cutoff, d	Unadjusted HR	Adjusted HR	95% CI of adjusted ratio	Unadjusted P, Cox regression
Cluster groups	45 (37/8)	NA	834	304	3.97	NA	1.4-11.0	.0081
hENT1	44 (36/8)	0.800	669	630	2.15	NA	NA	.12
hENT2	45 (35/10)	2.500	777	571	1.66	NA	NA	.27
hCNT3	45 (36/9)	0.400	834	304	5.41	4.67	1.52-14.4	.0007
dCK	45 (23/22)	4.500	630	1279	0.38	0.48	0.087-2.61	.035
CD73	45 (9/36)	0.025	257	777	0.32	0.40	0.081-1.98	.022
CN-II	43 (15/28)	1.000	322	834	0.530	NA	NA	.18
dNT-I	45 (10/35)	0.750	485	834	0.350	0.45	0.078-2.59	.042

NA indicates not applicable.

median TDP of 834 days, whereas patients with high hCNT3 mRNA levels had a median TDP of 304 days (HR 4.67; 95% CI 1.52-14.4). In a multivariate stepwise Cox regression analysis including the expression levels of each of the 7 genes, age, stage, sex, and pretreatment lymphocyte count, only hCNT3 was retained as a significant predictor of TDP (HR 4.67; $P < .01$).

Fludarabine-treated subjects with levels of hCNT3 mRNA below the cut point of 0.4 were more likely to achieve complete response (25 [69%] of 36 patients) than if hCNT3 mRNA levels were elevated (1 [11%] of 9 patients; Fisher exact test, $P = .002$). The mean hCNT3 expression was significantly lower in those patients who achieved a complete response (0.21 ± 0.08 [arbitrary units $\pm$ SEM]) than in those who did not achieve a complete response (0.55 ± 0.16; $P = .042$).

hCNT3 activity and localization in CLL cells

To determine if CLL cells exhibited the sodium-dependent plasma membrane hCNT3 activity, uptake of [^{3}H]-uridine was measured in cells obtained from 3 CLL patients with high levels of hCNT3 mRNA. Time courses of uridine uptake were measured in the presence and absence of sodium, with the addition of 100 μM dilazep to block uptake of uridine by the equilibrative nucleoside transporters. In the presence of dilazep, an inhibitor of equilibrative nucleoside transporters, the cellular uptake rate was zero, suggesting that there was no sodium-dependent uridine uptake through the plasma membrane over the time course measured. This was confirmed by uridine uptake rates that were identical in the presence and absence of sodium (Figure 5).

Immunohistochemistry for the hCNT3 protein was performed on an independent group of 16 lymph node samples derived from untreated CLL patients. In contrast to our positive control samples performed on pancreas tissue, where strong cytoplasmic staining for hCNT3 was observed in all islet cells, CLL samples had variable hCNT3 immunostaining (Figure 6). Cytoplasmic immunostaining was universally present in the prolymphocyte populations (composing 10% to 40% of cells) of each of the 16 samples. However, the small cell component, composing 60% to 90% of the malignant cells, had variable immunostaining. Six of the 16 samples exhibited cytoplasmic immunostaining in the small cells, whereas the remaining 10 cases had no detectable immunostaining in small cells. Dual immunohistochemical staining for CD3 and hCNT3 was performed and confirmed that hCNT3-positive cells were CD3$^-$ and therefore of B-cell lineage (data not shown).

To study these samples with a higher sensitivity imaging technique, confocal microscopy for the hCNT3 protein was performed on 3 independent samples derived from fludarabine-naive patients with CLL. Confocal microscopy demonstrated clearly detectable hCNT3 protein in all CLL cells. In the representative study shown in Figure 7, the IgM isotype control antibody resulted in a minimal signal, whereas the hCNT3 antibody showed intense cytoplasmic staining. These 3 CLL samples were tested for hCNT3 RNA expression and all 3 had low but detectable levels of hCNT3 message (0.02, 0.06, and 0.38) RT-PCR values for $2^{-(\Delta\Delta CT)}$.

Discussion

Numerous independent prognostic factors have been identified to differentiate good from poor prognosis CLL patient populations,
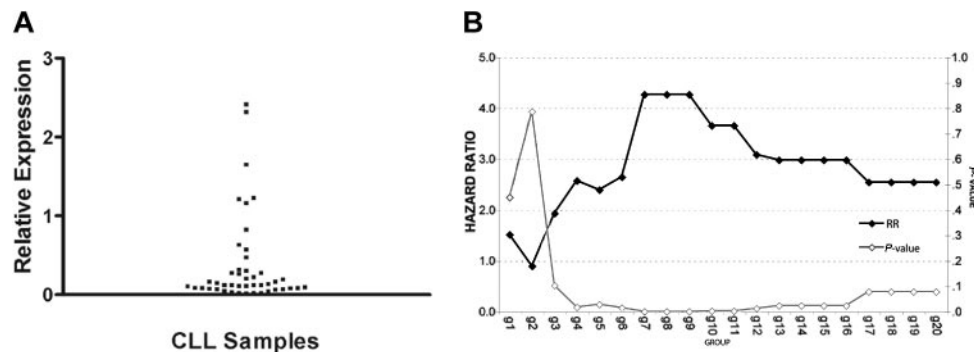

Figure 3. hCNT3 expression. (A) Scatter plot of hCNT3 expression. The distribution of hCNT3 expression among 45 samples of CLL is demonstrated in this graph. The expression of hCNT3 related to reference RNA levels is expressed in arbitrary PCR units. (B) Maximized significance of difference: hCNT3 expression dichotomization. In order to determine the optimal cut point value to maximize the significance of the difference between groups, the hCNT3 dataset was analyzed for each of 20 cut point groups (g1-g20), Kaplan-Meier curves were constructed, and log-rank analysis was performed. The scale on the left axis represents the log-rank–derived relative risk (♦), whereas the scale on the right represents statistical significance (P value; ◇). The curves separated maximally in groups 7, 8, and 9, corresponding to a hCNT3 expression value of 0.4 (arbitrary PCR units, see Figure 4).
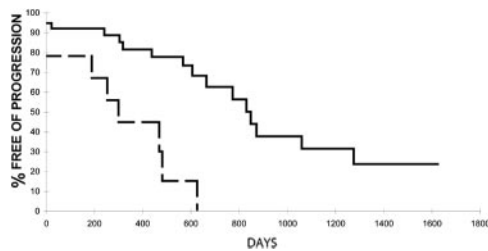
Figure 4. Time to disease progression dichotomized by hCNT3 expression. Kaplan-Meier analysis demonstrates that those patients with a high hCNT3 expression of at least 0.4 (arbitrary PCR units, - - -) had a substantially shorter time to disease progression after fludarabine therapy compared with those with levels less than 0.4 (arbitrary PCR units, —). The difference is significant with a hazard ratio of 4.67 (adjusted; $P = .0007$).

Figure 5. Uptake of uridine by CLL cells in the presence and absence of dilazep and sodium. Freshly purified CLL cells were exposed to 10 μM ^{3}H-uridine for the time periods indicated and uptake was measured in the following conditions: presence of extracellular sodium without dilazep (■); presence of extracellular sodium with 100 μM dilazep (●); absence of extracellular sodium with 100 μM dilazep (○). Each point represents the mean ± SEM of a single representative experiment performed in triplicate. Error bars are not shown where smaller than the data point.

but most chemotherapeutic decisions are still based upon prognostic groups defined by the Binet[18] or Rai[27] staging systems rather than a validated predictive assay.[28] Although the ex vivo differential staining cytotoxicity (DiSC) assay[29] has been used to identify fludarabine-resistant CLL patient populations,[30-32] this assay is not widely used due to its requirement for purification of CLL cells and 48-hour fludarabine exposures. Because no molecular predictive assay is available, we undertook this study of the expression of genes encoding key determinants of intracellular accumulation of fludarabine to determine if one or more might be predictive of fludarabine sensitivity.

In the present study, an unsupervised cluster analysis of the expression patterns of 7 genes encoding nucleoside transporter proteins and enzymes of nucleoside metabolism was performed. This analysis, performed without training algorithms and blinded to clinical outcomes, nonetheless identified 2 groups with markedly different clinical outcomes after fludarabine therapy (Figures 1-2; Table 3). This magnitude of the observed outcome differences, with a highly statistically significant hazard ratio of 3.4, suggests that the expression profile for these 7 genes may be a novel prognostic assay for fludarabine-treated CLL. Although this result was consistent with the hypothesis that expression profiling identifies a molecularly defined CLL population with more aggressive disease, we found no statistical association between cluster designation and the typical clinical markers of disease aggressivity (eg, high WBC count, high stage). Rather, we favor the hypothesis that the expression of transporters and metabolism enzymes is linked mechanistically with fludarabine activity and thereby exerts a direct effect on cellular fludarabine sensitivity. Supporting this
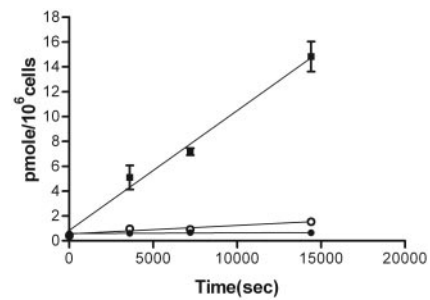
hypothesis is the observation that low dCK expression, as expected from preclinical studies showing fludarabine resistance,[33] was associated with inferior treatment outcomes in our study. Additionally, expression levels of 4 of the 7 individual genes (hCNT3, dCK, CD73, and dNT-1) showed univariate statistical associations with TDP after fludarabine therapy when optimized cut points were used (Table 3). In agreement with another report, message levels of hENT1 and hENT2 were not statistically associated with fludarabine cytotoxicity.[16]

The most statistically significant indicator of clinical fludarabine resistance was a high level of hCNT3 expression (Figure 4; Table 3), with high hCNT3 expression associated with a statistically significant hazard rate for progression of 4.67, even when adjusted for optimum cut point selection. On multivariate stepwise Cox regression analysis of expression levels of the 7 genes, age, stage, sex, and pretreatment lymphocyte count, the only predictor of TDP was hCNT3 (HR 4.67; $P < .01$). Additionally, high hCNT3 expression was associated with a significantly lower rate of complete response to fludarabine (11% vs 69%; $P = .002$). The recently identified hCNT3 sodium-dependent transporter gene encodes an inwardly directed sodium-coupled plasma membrane nucleoside transporter.[15] hCNT3 is unique among human CNTs in exhibiting a 2:1 Na$^+$/nucleoside coupling ratio and an ability to substitute H$^+$ for Na$^+$.[15]

Our original hypothesis was that higher nucleoside transporter expression would lead to more efficient fludarabine intracellular
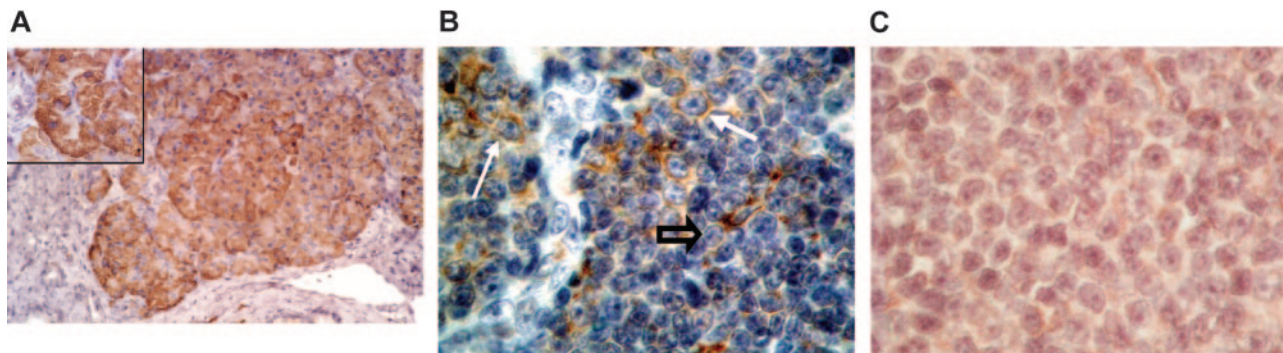

Figure 6. Immunohistochemistry for hCNT3 in pancreas tissue and lymph nodes from CLL patients. (A) Normal pancreas tissue showing the intense positive cytoplasmic staining for hCNT3 exhibited by pancreatic islet cells (original magnification × 25; inset × 40). (B) This CLL case shows pseudofollicles with prolymphocytes (white arrows) that were positive for hCNT3 immunostaining, whereas the small cell component (black open arrow) shows no immunostaining (original magnification × 40). (C) This CLL case again shows cytoplasmic staining in the scattered prolymphocytes, whereas small cells show detectable cytoplasmic immunostaining (original magnification × 40). Images were captured with a Nikon Eclipse E 680 microscope by Nikon View V3.0 software (Nikon, Melville, NY) using a Nikon 40 × lens with a 0.65 aperture.
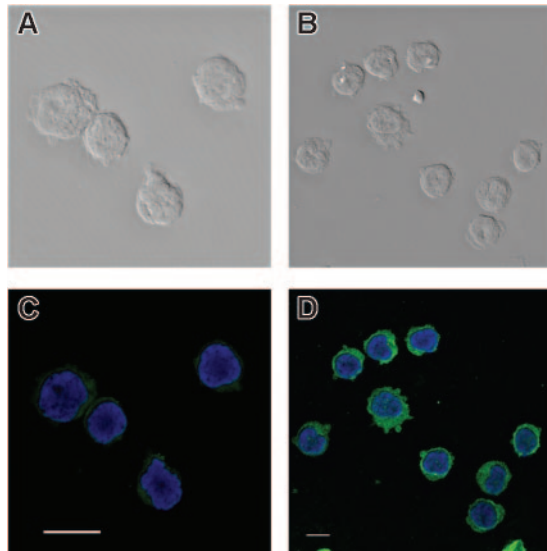
Figure 7. Confocal photomicrograph for hCNT3 in CLL cells. (A,C) Background staining of CLL cells reacted with an IgM isotype control antibody shown in phase contrast (A) or fluorescent confocal microscopy (C). (B,D) CLL cells reacted with hCNT3 monoclonal antibody shown in phase contrast (B) or fluorescent confocal microscopy (D) illustrating intense cytoplasmic staining by this antibody.

accumulation and would be seen in fludarabine-sensitive populations; the strong association of high hCNT3 expression with relative fludarabine insensitivity was an unexpected finding. To explore how hCNT3 might be involved in conferring fludarabine resistance, we assessed hCNT3 plasma membrane activity in CLL cells from 3 fludarabine-naive patients. Although these CLL cells exhibited high levels of hCNT3 mRNA, we found no evidence of sodium-dependent plasma membrane uptake of radiolabeled uridine, a good substrate for the hCNT3 protein (Figure 5). We thereby conclude that functional plasma membrane hCNT3 was not detectable in these fludarabine-naive hCNT3-expressing CLL samples. This result is consistent with another report, where in CLL samples derived from 20 patients, sodium-dependent fludarabine transport was not identified.[16]

To determine whether hCNT3 protein was present in CLL, we performed immunohistochemistry using a recently developed and validated monoclonal antibody against hCNT3.[26] Positive controls were provided by studies of pancreas, where cytoplasmic hCNT3 was readily detectable in islet cells (Figure 6A). We studied 16 lymph node samples derived from treatment-naive CLL patients. All samples demonstrated cytoplasmic immunostaining of the prolymphocyte cell population (which composed 10%-40% of the lymphoma cells; Figure 6C). Six of the 16 samples also showed cytoplasmic immunostaining in the small cell population (Figure 6B). To further corroborate the localization of the hCNT3, confocal microscopy was performed. In each of the CLL samples tested, hCNT3 was identified and localized in the cytoplasm (Figure 7). Using cell fractionation and immunoblotting, we have recently shown hCNT3 to be associated with internal cellular membranes

(C.E.C., unpublished observation, March 2004). In aggregate, these studies indicate that while hCNT3 is present in CLL cells, this protein is not localized to the plasma membrane of CLL cells and, unlike the equilibrative nucleoside transporters, does not contribute to the intracellular uptake of fludarabine.

We conclude that although RNA expression of hCNT3 identified a fludarabine-resistant population of CLL, the mechanism remains unclear. Plasma membrane transport activity of the hCNT3 protein was not detected in this study and the hCNT3 protein was only identified in the cytoplasm of CLL cells. Possible explanations for the strong relationship between hCNT3 gene expression and fludarabine resistance include the following: (1) the hCNT3 gene is coordinately regulated with other genes that mediate fludarabine resistance; (2) hCNT3 RNA expression is simply a biologic marker of a distinct CLL subpopulation with intrinsic fludarabine resistance, perhaps similar to novel subpopulations of CLL identified by global gene-expression studies[34] or by analysis of somatic hypermutation of Ig genes[35,36]; and (3) baseline hCNT3 gene expression may relate to the abundance of cytoplasmic hCNT3 protein, where, if localized to the membranes of an intracellular organelle such as mitochondria, it may directly modulate fludarabine toxicity. Because hCNT3 plasma membrane activity is highly inducible by differentiating agents in some hematologic cell lines,[15,37] it is also possible that hCNT3 protein may be produced or directed to the plasma membrane in response to fludarabine exposure. Increased hCNT3 activity at the level of the plasma membrane might then confer fludarabine resistance by providing "salvage" nucleoside transport capability to minimize the intracellular nucleoside pool depletion induced by fludarabine. Further studies are underway to distinguish among the above hypotheses. We do not believe that the variability in expression of hCNT3 derived from blood samples of CLL patients is simply a reflection of the abundance of circulating prolymphocytes; although prolymphocytes comprise a substantial component of the malignant cells in lymph nodes of CLL patients, none of our CLL cases had more than 10% circulating prolymphocytes on peripheral smears.

In summary, the analysis of expression profiles of genes that encode proteins responsible for fludarabine transport and metabolism may be used to identify those patients who derive limited benefit from fludarabine therapy. This implies that the early steps of plasma membrane permeation via nucleoside transporters and fludarabine metabolism are clinically relevant determinants of drug cytotoxicity. Additional studies are warranted to provide mechanistic explanations for the observed strong relationship between hCNT3 expression and clinical fludarabine resistance.

Acknowledgments

References

1. O'Brien S, Kantarjian H, Beran M, et al. Results of fludarabine and prednisone therapy in 264 patients with chronic lymphocytic leukemia with multivariate analysis-derived prognostic model for response to treatment. Blood. 1993;82:1695-1700.

2. Spriano M, Chiurazzi F, Liso V, et al. Multicentre prospective randomized trial of fludarabine versus chlorambucil and prednisone in previously untreated patients with active B-CLL. Hemat Cell Ther. 2000;42:86.

3. Rai KR, Peterson BL, Appelbaum FR, et al. Fludarabine compared with chlorambucil as primary therapy for chronic lymphocytic leukemia. N Engl J Med. 2000;343:1750-1757.

4. Leporrier M, Chevret S, Cazin B, et al. Randomized comparison of fludarabine, CAP, and ChOP in 938 previously untreated stage B and C chronic lymphocytic leukemia patients. Blood. 2001;98:2319-2325.

5. Johnson S, Smith AG, Loffler H, et al. Multicentre prospective randomised trial of fludarabine versus cyclophosphamide, doxorubicin, and prednisone (CAP) for treatment of advanced-stage

chronic lymphocytic leukaemia: The French Co-operative Group on CLL. Lancet. 1996;347:1432-1438.

6. Sorensen JM, Vena DA, Fallavollita A, Chun HG, Cheson BD. Treatment of refractory chronic lymphocytic leukemia with fludarabine phosphate via the group C protocol mechanism of the National Cancer Institute: five-year follow-up report. J Clin Oncol. 1997;15:458-465.

7. Pott-Hoeck C, Hiddemann W. Purine analogs in the treatment of low-grade lymphomas and chronic lymphocytic leukemias. Ann Oncol. 1995; 6:421-433.

8. Plunkett W, Gandhi V, Huang P, et al. Fludarabine: pharmacokinetics, mechanisms of action, and rationales for combination therapies. Semin Oncol. 1993;20:2-12.

9. Plunkett W, Gandhi V. Cellular pharmacodynamics of anticancer drugs. Semin Oncol. 1993;20:50-63.

10. Consoli U, El-Tounsi I, Sandoval A, et al. Differential induction of apoptosis by fludarabine monophosphate in leukemic B and normal T cells in chronic lymphocytic leukemia. Blood. 1998;91: 1742-1748.

11. Pettitt AR, Sherrington PD, Cawley JC. Role of poly(ADP-ribosyl)ation in the killing of chronic lymphocytic leukemia cells by purine analogues. Cancer Res. 2000;60:4187-4193.

12. Sandoval A, Consoli U, Plunkett W. Fludarabine-mediated inhibition of nucleotide excision repair induces apoptosis in quiescent human lymphocytes. Clin Cancer Res. 1996;2:1731-1741.

13. Galmarini CM, Mackey JR, Dumontet C. Nucleoside analogues: mechanisms of drug resistance and reversal strategies. Leukemia. 2001;15:875-890.

14. Gati WP, Paterson ARP, Belch AR, et al. Es nucleoside transporter content of acute leukemia cells: role in cell sensitivity to cytarabine. Leuk Lymphoma. 1998;32:45-54.

15. Ritzel MW, Ng AM, Yao SY, et al. Molecular identification and characterization of novel human and mouse concentrative Na+-nucleoside cotransporter proteins (hCNT3 and mCNT3) broadly selective for purine and pyrimidine nucleosides (system cib). J Biol Chem. 2001;276:2914-2927.

16. Molina-Arcas M, Bellosillo B, Casado FJ, et al. Fludarabine uptake mechanisms in B-cell chronic lymphocytic leukemia. Blood. 2003;101:2328-2334.

17. Plunkett W, Saunders PP. Metabolism and action of purine nucleoside analogs. Pharmacol Ther. 1991;49:239-268.

18. Binet JL, Auquier A, Dighiero G, et al. A new prognostic classification of chronic lymphocytic leukemia derived from a multivariate survival analysis. Cancer. 1981;48:198-206.

19. Cheson BD, Bennett JM, Grever M, et al. National Cancer Institute-sponsored Working Group guidelines for chronic lymphocytic leukemia: revised guidelines for diagnosis and treatment. Blood. 1996;87:4990-4997.

20. ABI PRISM 7700 Sequence Detection System User Bulletin no. 2. Foster City, CA: Applied Biosystems; 1997.

21. Fink L, Seeger W, Ermert L, et al. Real-time quantitative RT-PCR after laser-assisted cell picking. Nat Med. 1998;4:1329-1333.

22. Reiman T, Graham KA, Belch AR, et al. Mechanisms of resistance to nucleoside analogue chemotherapy in mantle cell lymphoma: a molecular case study. Leukemia. 2002;16:1886-1887.

23. Eisen M. Cluster and TreeView Manual. Stanford University, CA; 1999.

24. Eisen MB, Spellman PT, Brown PO, Botstein D. Cluster analysis and display of genome-wide expression patterns. Proc Natl Acad Sci U S A. 1998;95:14863-14868.

25. Hollander N, Sauerbrei W, Schumacher M. Estimating the effect of a prognostic or risk factor after selection of an "optimal" cutpoint. Stat Med. 2004;23:1701-1713.

26. Lang TT. Studies of recombinant and native human concentrative nucleoside transporters and their role in nucleoside pharmacology and adenosine signaling. Edmonton, AB. University of Alberta Press; 2003.

27. Rai KR, Sawitsky A, Cronkite EP, Chanana AD, Levy RN, Pasternack BS. Clinical staging of chronic lymphocytic leukemia. Blood. 1975;46: 219-234.

28. Rozman C, Montserrat E. Chronic lymphocytic leukemia. N Engl J Med. 1995;333:1052-1057.

29. Weisenthal LM, Marsden JA, Dill PL, Macaluso CK. A novel dye exclusion method for testing in vitro chemosensitivity of human tumors. Cancer Res. 1983;43:749-757.

30. Bosanquet AG, Bell PB. Enhanced ex vivo drug sensitivity testing of chronic lymphocytic leukaemia using refined DiSC assay methodology. Leuk Res. 1996;20:143-153.

31. Bosanquet AG, Johnson SA, Richards SM. Prognosis for fludarabine therapy of chronic lymphocytic leukaemia based on ex vivo drug response by DiSC assay. Br J Haematol. 1999;106:71-77.

32. Mason JM, Drummond MF, Bosanquet AG, Sheldon TA. The DiSC assay: a cost-effective guide to treatment for chronic lymphocytic leukemia? Int J Technol Assess Health Care. 1999;15:173-184.

33. Bai L, Yamaguchi M, Tatsumi M, Kon K, Brautigam M. Mechanisms responsible for resistance of sublines derived from leukemia cell lines to an antitumor agent 9-beta-D-arabinofuranosyl-2-fluoroadenine. J Cancer Res Clin Oncol. 1998; 124:367-373.

34. Stratowa C, Loffler G, Lichter P, et al. CDNA microarray gene expression analysis of B-cell chronic lymphocytic leukemia proposes potential new prognostic markers involved in lymphocyte trafficking. Int J Cancer. 2001;91:474-480.

35. Stevenson FK, Sahota SS, Ottensmeier CH, Zhu D, Forconi F, Hamblin TJ. The occurrence and significance of V gene mutations in B cell-derived human malignancy. Adv Cancer Res. 2001;83:81-116.

36. Hamblin TJ, Davis Z, Gardner A, Oscier DG, Stevenson FK. Unmutated Ig V(H) genes are associated with a more aggressive form of chronic lymphocytic leukemia. Blood. 1999;94:1848-1854.

37. Tortora G, Yokozaki H, Pepe S, Clair T, Cho-Chung YS. Differentiation of HL-60 leukemia by type I regulatory subunit antisense oligodeoxynucleotide of cAMP-dependent protein kinase. Proc Natl Acad Sci U S A. 1991;88:2011-2015.